# Continuous Particle Separation Using Inertial Focusing in a Dean Flow Driven Microchannel

UTKU SONMEZ [1, 2], SAMIR JABER [1, 2], LEVENT TRABZON [1, 2, 3]

[1] Mechanical Engineering Department, Istanbul Technical University, Istanbul, Turkey
[2] ITU-MEMS Research Center, Istanbul Technical University, Istanbul, Turkey
[3] ITUnano Research Center, Istanbul Technical University, Istanbul, Turkey

PLEASE SCROLL DOWN FOR ARTICLE

# CONTINUOUS PARTICLE SEPARATION USING INERTIAL FOCUSING IN A DEAN FLOW DRIVEN MICROCHANNEL

UTKU SONMEZ [1, 2], SAMIR JABER [1, 2], LEVENT TRABZON [1, 2, 3] *

[1] Mechanical Engineering Department, Istanbul Technical University, Istanbul, Turkey
[2] ITU-MEMS Research Center, Istanbul Technical University, Istanbul, Turkey
[3] ITUnano Research Center, Istanbul Technical University, Istanbul, Turkey

**Abstract.** The processes separation and focusing of microparticles in microfluidic devices have developed to be an essential part of several applications in biomedical, clinical, chemical, environmental and engineering domains. Regarding their part in the diagnosis and treatment of diseases, such as cancer, particle separation processes play an important role as they bring about earlier diagnosis [1] beyond the one provided by customary medical and clinical treatment. Metastatic cancer, for instance, has long been under study and research, with the aim to find the best way to detect and cure such disease. Microfluidics offer a relatively efficient technique in particle separation. The presence and frequency of circulating tumor cells (CTCs) in blood are critical in the course of early detection of cancer. However, such cells are rare and infrequent [2], which makes it challenging to detect them easily and with precision. In this paper, we illustrate the separation of particles in a spiral microchannel based on inertial forces and differential migration. This passive microfluidic device can deliver the separation of particles based on their sizes. It's made of four loops with an initial radius of curvature of 2 cm, a channel width of 500 μm, and a height of 50 μm. Systematic analysis, the manufacturing process, simulations and the methodology of this microfluidic system are presented here alongside the experimentation. The straightforwardness, material and productivity of this design makes it a perfect model for lab-on-a-chip (LOC) or micro total analysis systems (μTAS), as it allows for continuous separation applications.

## INTRODUCTION

The separation of microparticles, whether biological or synthetic they are, is an essential process for various applications in the domains of biology, medicine, healthcare and manufacturing. In particular, the isolation of circulating tumor cells (CTCs) in blood is crucial, as they directly contribute to cancer metastasis, yet challenging, taking into consideration their rarity in bloodstreams. Conventional approaches for filtration and isolation of microparticles depend on the usage of a membrane filter, and on particle kinesis or positioning under the effect of various external forces. These approaches are limited by the aspect that the flow is to be laminar, and by the size of pores in the membrane, which renders these traditional procedures inefficient in terms of separating a various number of microparticles. Besides, the use of membranes in filtration suffers an issue of clogging and membrane fouling, in addition to its being a costly process. Consequently, new separation methods of particles and biological cells have been established and developed exclusive of the use of membranes. Some of the recent membrane-less separation processes include field-flow fractionation (FFF) [3], pinched flow fractionation (PFF) [4], hydrodynamic chromatography (HDC) [5], sedimentation,

electrophoresis [6], dielectrophoresis [7], centrifugation [8] and inertial focusing [9]. A majority of these separation techniques, nonetheless, function with stopped-flow as opposed to continuous flow, necessitating the introduction of specific finite sample volumes. However, lab-on-a-chip (LOC) applications are supposed to result in rapid investigation and identification, leading to the requirement of continuous particle separation [10]. Such a condition brings about constraints for the separation techniques above, as they are associated with long analysis periods, complex manufacturing and complicated integration with customary LOC elements. Plus, the use of externally applied forces may result in the damage of biological cells. Accordingly, passive membrane-less microfluidic systems have been developed in order to operate without being constrained with such limitations. Two significant passive particle separation techniques that have been currently displayed and operated are centrifugal-based separation and inertial focusing in curvilinear microchannels. These processes are advantageous in terms of being membrane-less, allowing for continuous flow processing, and non-requiring of external forces, hence resulting in an easier fabrication and application on wide range of particles and

---

* Corresponding author: Levent Trabzon
E-mail: trabzonl@itu.edu.tr

biological molecules. The channels provided for these processes are fabricated with respect to specifically constructed geometries, out of which the most significant are spiral, described by [11], and asymmetric curvilinear geometries, accounted for by [12] According to the work of in asymmetric curvilinear channels, particles having a diameter larger than 0.07 the microchannel's hydraulic diameter (i.e. $a_p / D_H > 0.07$ where $a_p$ is the particle diameter and $D_H$ is the hydraulic diameter) are likely to occupy a single equilibrium position. Using this principle, they were able to separate 10 μm particles from 2 μm particles, in which the latter remained scattered throughout the channel, while the former focused into a concentrated stream to be collected alone.

In terms of isolating CTCs, as described by [13]. It is necessary to set specific points whilst designing and assessing the microfluidic system. These points include high efficiency (separating all CTCs from blood), high throughout (processing large sample volume in short time), and high purity (collecting only CTCs without the other cells), in addition to cell enrichment and minimization of cell clogging [13]. In this work, we perform a continuous size-based separation of microparticles using inertial focusing and Dean flow in a microfluidic channel of a spiral geometry, with no use of external forces. This geometry is schematically shown in Figure 1.
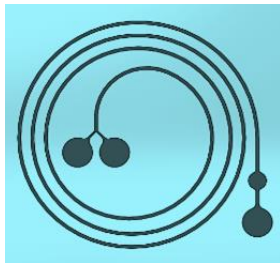


Fig. 1. A schematic of the spiral microchannel under study.

In this configuration, we were able to achieve relatively high efficiency of particle focusing by means of inertial lift forces that push the particles away from the channel's center and wall, and Dean drag that transfers the particles along the two Dean vortices developed in the upper and lower halves of the channel. In a previous study of the spiral microchannel, [11] have shown that large sized particles concentrate into a focused equilibrium position near the inner wall of the channel [11]. In our study, as expected, large sized particles were also concentrated near to the inner boundary with high focus quality, as the smaller sized particles scattered throughout the channel. Thus, in this paper, we illustrate our work from point one, as in setting our hypothesis, to manufacturing our microfluidic system, performing our analyses, and obtaining our results and conclusions.

## LITERATURE REVIEW

The process of operation is based inertial focusing. Several studies by others have been performed previously on this process [9], [11], [14]. Basically, inertial focusing takes place by means of hydrodynamic forces that amend the movement of particles towards focusing at an equilibrium position throughout the channel. These forces are described as drag forces and lift forces. As the particle-carrying fluid flows across the spiral channel, it undergoes a centrifugal acceleration due to the curvilinear characteristic of the channel. This give rise to the formation of two Dean vortices (secondary flow) rotating in opposite manner in the top and bottom halves of the channel. This flow's magnitude can be represented by a dimensionless Dean number (De), in which

$$De = Re \sqrt{\frac{D_H}{2R}}$$

where $Re$ is the flow Reynolds number, and $R$ is the radius of curvature [m] of the channel. $De$ increases with smaller $R$ (i.e. higher curvature). As $R \rightarrow \infty$, the microchannel becomes straight and $De = 0$, which shows the nonexistence of Dean flows. $De$ also is proportional to $Re$ and $D_H$, where it increases, respectively, with increasing flow velocity and with larger cross-sectional area of the channel. Due to the present Dean flow in the channel, the particles flowing through undergo a Dean drag force $F_D$, which causes them to travel along the Dean vortices independent on their particle size. This drag force can be described by

$$F_{drag} = (5.4 \times 10^{-4}) \pi \mu De^{1.63} a_p \ [N] \qquad (2)$$

where $\mu$ is the dynamic viscosity of the fluid. This shows the direct proportionality between the drag force and the particle size.

Besides the drag force, the flowing particles experience inertial lift forces and pressure forces. Considering the parabolic figure of the velocity profile in Poisseuille flow, a resulting shear-induced inertial lift force $F_{SL}$ pushes the particles away from the center of the microchannel. As the particles approach the walls, an asymmetric disturbed flow region is generated about the particles, resulting in a wall-induced inertial lift force $F_{WL}$ which directs the particles away from the wall. At the point where the magnitudes of these two forces balance, the particles are likely to occupy that point as an equilibrium position to follow through downstream, or continue to flow along the Dean vortices. Formulated by Asmolov [15], the net lift force can be represented by

$$F_{inertial} = \rho G^2 C_L a_p^4 \ [N] \qquad (3)$$

where $\rho$ is the density of the fluid medium, $G$ is the rate of shear of the fluid $(G = U_{max}/D_H)$, $U_{max}$ being the maximum velocity of the fluid and $D_H$ the hydraulic diameter, $C_L$ is the lift coefficient approximated to an average value of 0.5, and $a_p$ is the particle diameter. This shows that the inertial forces increase with

the particle size much faster than the Dean drag (to a power of 4). As stated by [9], [11] at low Reynolds number, the number of equilibrium positions in a rectangular microchannel where the lift forces balance each other decreases to four. [9] By adding a Dean drag force, this number becomes only one near to inner boundary of the Microchannel [16].

## METHODOLOGY
### Microchannel Design and Fabrication

The spiral microchannel was manufactured in a Polydimethylsiloxane (PDMS, Sylgard 184, Dow Corning). The design was first generated on a mask by laser lithography (Heidelberg DWL 66FS). It is made of a 4-loop spiral geometry with one inlet and two bifurcating outlets. The initial radius of curvature is 2 mm, the channel width is 500 μm and height is 50 μm. The microchannel was fabricated using soft lithography. A polished hydrophobic-rendered Si-wafer was covered with a 50 μm thick Su-8 photoresist (3000, Microchem. Corp.) Using a Spin Coater (Laurell WS-400B). Using typical photolithography, the design was patterned on the Si-wafer in a mask aligner (OAI Hybralign Series 200). The PDMS prepolymer, initially mixed at a ratio of 10:1 with the curing agent and then degassed in a vacuum chamber (Sheldon Manufacturing, Inc.), was poured onto the Su-8 mold and baked at 90°C (Figure 2).
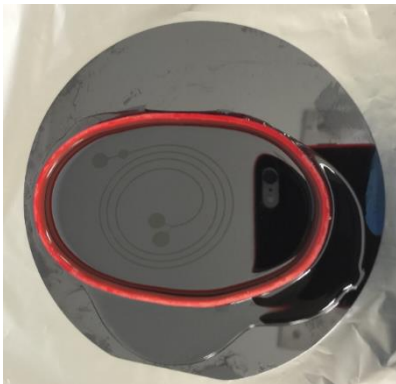


Fig. 2. Poured PDMS over the heater where it is cured in 30 minutes at 90°C.

Afterwards, the PDMS was detached from the mold, three fluid access holes (one inlet and two outlets) were introduced, and the PDMS was bonded to a piece of glass by oxygen plasma bonding in a basic plasma cleaner (Harrick Plasma) to finalize the microchannel fabrication.

### Computer Simulations

In order to realize the process theoretically, computer simulations using Comsol Multiphysics 5.0 were done, describing the laminar flow of a fluid streaming across the spiral microchannel, and the tracing of particles within the flow. The study of the flow demonstrates the change in velocity and

pressure throughout different positions of the channel cross-section, which shows the effect of the secondary Dean flow.



Fig. 3. The spiral microchannel following its manufacturing in PDMS.

In the particle tracing study, the focusing of particles was investigated, where the degree of focusing and the location within the channel at which the focus takes place and remains as such were determined. These simulations were an initial step towards comprehending the course of particle separation in hand.
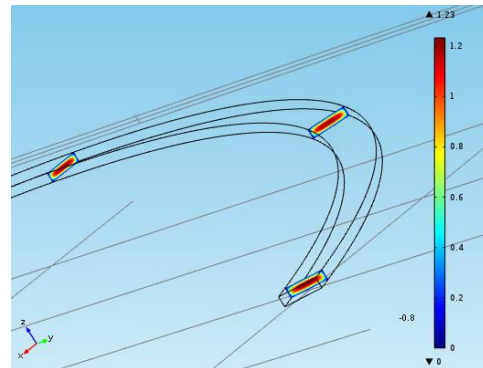


Fig. 4. Velocity field in spiral microchannel geometry at 0.7 ml/min⁻¹.

### Experimentation

With the purpose of investigating the spiral microchannel's separation capability and efficiency, a number of continuous experiments were carried out, and assessed in comparison with previously done experiments in different relative studies. Water was used as the fluid to be passed through the microchannel. Using a 5 cc syringe pump, water was pumped from the outer inlet to the inner outlets, carrying 3 μm particles (red) and 9.9 μm particles (green), with various flow rates ranging between 0.3 ml.min⁻¹ and 2.5 ml.min⁻¹. During the experimental testing, high speed images of the microchannel were captured at different locations using a 12.8 megapixel cooled digital color camera (Olympus DP72) mounted on an epiflouorescence microscope (Olympus EX51). Around 400 images were taken and analyzed individually, and then the results were tabulated and analyzed. A brightness analysis was

performed using *Image J*, through which the optimal flow rate was determined. During this analysis, the brightness of the dispersed 3 μm particles was neglected as compared to that of the 9.9 μm particles, and considered as part of the background brightness. To perform this analysis, an empirical formula was developed relating the focus quality to the brightness intensity and the breadth of the focus. This relation is illustrated as

$$q_{focus} = \left(\frac{W_{channel}-\Delta x_{focus}}{W_{channel}-a_{particle}}\right) \cdot \left(\frac{\Sigma V_{focus}}{\Sigma V_{all}}\right) \qquad (4)$$

Where $W_{channel}$ is the channel width [μm], $a_{particle}$ is the particle diameter [μm], $\Delta x_{focus}$ is the focus width [μm], $\Sigma V$ is the sum of brightness intensity values and $q_{focus}$ is the normalized focus quality. The focus quality increases as more particles concentrate into one focus line, thus producing a higher brightness intensity. The ideal focus quality of 1 is when all the 9.9 μm particles line up in a single focus line of width equal to the particle size. This focus quality represents the efficiency of the separation process, in which the higher the focus quality, the more particles are collected separately, thus resulting in a higher efficiency.
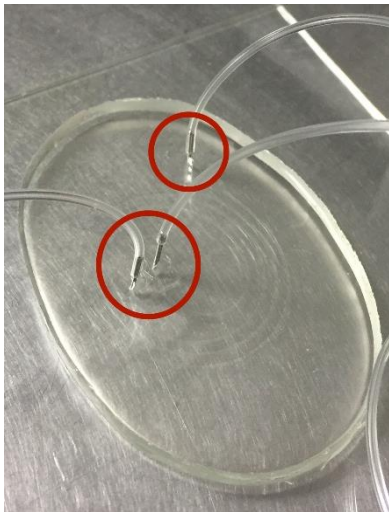


Fig. 5. The spiral microchannel during operation.

## RESULTS

The openings to where the tubings are connected (shown in red) are the inlet and outlets, respectively in (Figure 5). Upon the experiments done to test our superposition assumption images taken from just before the bifurcation are examined by using Image J for the light intensity analysis. At this point, a line perpendicular to the focus line was drawn from the outer wall to the inner wall of the microchannel, and the light intensity throughout this line was plotted after properly scaling its length to the channel width as 500 μm for spiral geometry before the bifurcation (Figure 6). The peak section seen on the plot corresponds to the focus line. By measuring the bottom span of the peak, the width of the focus line was calculated. In an ideal situation this value would correspond to the diameter of the

focused particle which is 9.9 μm in this case since the focus line would be composed of a single particle train. The second part of the normalized focus quality formula that we have developed, depicts the separation ability of the microchannel. Moreover, taking the integral of the plot, the total amount of large-size particles in the microchannel was estimated and compared to that within the focus line. Bearing in mind that the dispersed small red particles contribute to the background brightness, It was required to determine a reference brightness threshold in the plot that would neglect any effects that red particles could cause on the focus line quality (Figure 7). In other words, the brightness values that lied under this reference line were attributed to red particles, while the brightness values that surpassed it were automatically taken as green particles.
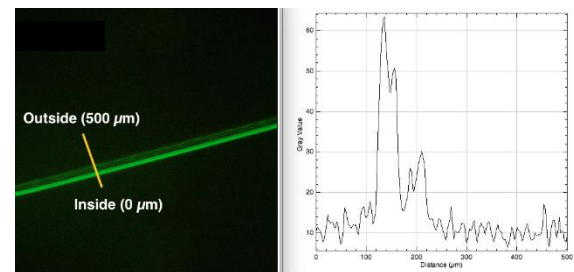


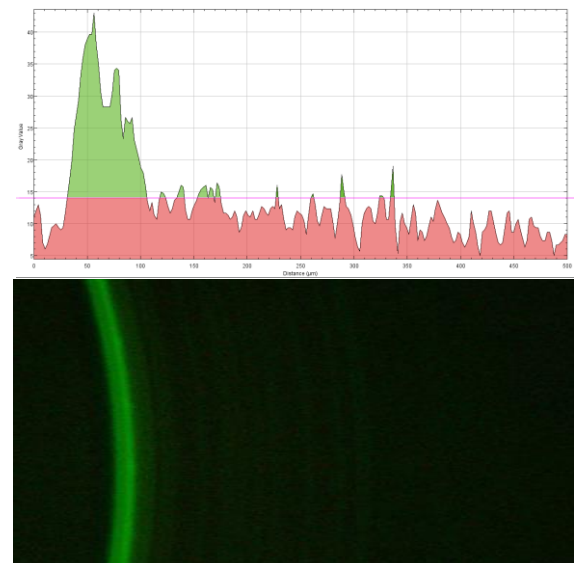Fig. 6. Light intensity throughout the cross section of the microchannel before the bifurcation.



Fig. 7. Analysis of the focus line by plotting light distribution throughout the channel cross section.

The magenta line shows the threshold value for the green particles in (Figure 7).Accordingly, the values obtained from the plot were tabulated, and the mentioned variables were calculated for different volumetric flow rates (Figure 8).
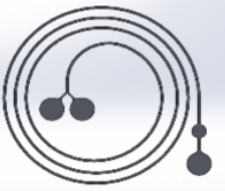
Fig. 8. Tabulated normalized focus quality values for spiral geometry at different flow rates.

The best results were obtained at 1.5 ml.min$^{-1}$ for the spiral geometry, 0.81. Herein, one should note that the normalized focus quality ratio that we derived not only contained the separation ratio, but also gave an initial idea about the narrowness of the focus line with respect to the channel width and the particle diameter (Figure 7). For this reason, the separation ratios of the microchannel were expected to be higher than its normalized focus quality while being in the same trend. At the flow rates less than 0.9 ml.min$^{-1}$ we did not observe significant focus formation. This is probably due to the insufficient contribution of the inertial forces and Dean flow drag at low velocities. As the velocity increases focus line tends to be more visible and narrow. When the flow rate is set to 1.5 ml.min$^{-1}$, we observed the narrowest and brightest focus line. Increasing the flow rate more then this values led to the dispersion of the particles in the focus line throughout the channel, which in turn decreased the normalized focus line quality. The dispersion of the particles is though to be due to higher scales of the Dean forces than the net inertial lift, which caused the particles to follow Dean vortices. The position of the focus line inside the microchannel also changes as the flow rate increases. At the flow rates less than 1.5 ml.min$^{-1}$, particles focus near the centerline. Then they immigrate through the inner sidewall by increasing flow rate. After 1.5 ml.min$^{-1}$, particles tend to move away from the inner sidewall before the dispersion. As the flow rate approaches to the optimum flow rate, shear-induced inertial lift forces becomes stronger since the velocity gradient between microchannels centerline and the inner sidewall increases. Thus, particles get closer to the inner sidewall. However, after the optimum flow rate, Dean vortices become dominant and carry the particles from inner sidewall through the microchannels

centerline. During the experiments we have never seen the focus formation of smaller (red) particles, since the net inertial lift force that affect on them was not sufficient to determine a focus line for them. Consequently, they were traveling throughout the microchannel cross section by following one of the Dean vortices. Lastly, the formation of focus line is determined by observing the behavior of the particles that contributes to the focus along the spiral pattern. To have a better idea, fluorescent images are taken from each loop of the spiral geometry (Figure 9). We observed continuous enhancement of the focus line quality approaching to the outlets. This result suggest that the length of the microchannel can be increased to have better focus qualities since the formation of the focus line could continue if extra distance is provided.
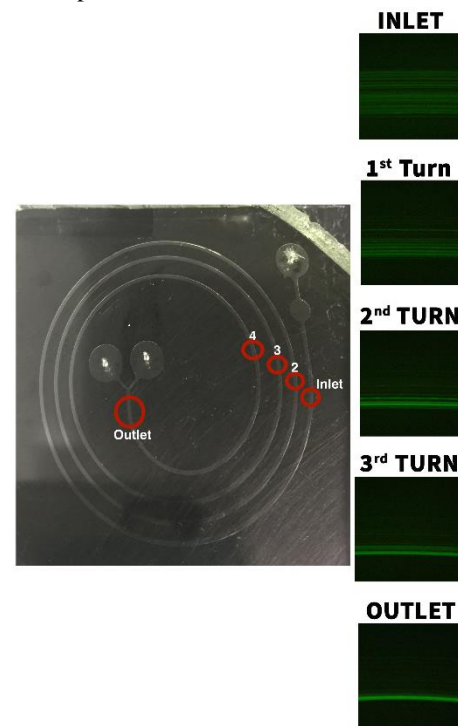


Fig. 9. The formation of focus line in a spiral microchannel. Images are taken at 1.5 ml.min$^{-1}$ from each turn.

Results that we have obtained are also compatible with the previous research studies done on spiral microchannels. Kuntaegowdanahalli et al. shared the similar focus line formation trend in their articles [17]. To sum up, we have demonstrated that our microchannel geometry allows for better separation performance than the other two microchannel geometries. Plus, the optimum flow rate of 1.5 ml.min$^{-1}$ results in a quite high throughput that would considerably reduce the process time.

**DISCUSSION AND CONCLUSION**

According to the experimental results that we have obtained, the spiral geometry seems to have a good optimum focus quality which would lead to a better separation or

enrichment performance depending on the desired process than its peer microfluidic devices. As well as, it maintains an acceptable portion of its optimum separating ability at flow rates varying around 1.5 ml.min$^{-1}$. This characteristic implies the robustness of the microchannel geometry which is not affected by the fluctuation of the flow rate which is an important problem for other microfluidic separation techniques that work with fluctuated flow rates due to low volumetric flow rates. As a result, it is safe to say that while spiral geometry tolerates possible shortcomings of not being supplied a fluid flow at its optimum operation point.

In general, our experiment has shown that the microchannel geometries can be used for continuous inertial separation. By doing so, improved microchannel geometries can be designed to have better separation, better enrichment and higher throughput. Furthermore, compactness of the microchannel can be amended by increasing the particle migration and decreasing the required time for focus formation or simply reducing the footprint of the device. More experiments are to be done to evaluate the properties of this geometry. Essentially, experiments will be performed with living cells instead of polystyrene particles to see their response to the microchannels hydrodynamic forces on their elastic structure. This matter, generally, reduces the quality of the focus line, and thus the separation ability of the microchannel, not only because of their elastic membranes that deform under such flow conditions, but also because of the high deviation of their diameters. In case of the successful results that would be obtained from cell lines, separation of cells from the whole blood should be experimented. Regarding this issue, there is a considerable amount of research that has been done with spiral microchannels [2].

At this point, separation of Circulating Tumour Cells (CTCs) from the whole blood seems to be the center of interest due to the ease of separating them by using their size difference and the importance of the topic as it leads to the earlier diagnosis of various metastatic cancer diseases. However, the main disadvantage of this methodology is that the separation process is specifically optimized for a particular course of separation. In other words, to be able to apply this methodology for different cells or particles, it is required to redesign the various parameters of the microchannel such as height, width, radius of curvature and ideal flow rate. On the other hand, transforming the inertial microchannel technology into a commercial LOC device is possible, and this can be done only for a particular need where each type of microchannel with different dimensional parameters can be used merely to realize a particular task (e.g. separation of 16 μm metastatic breast cancer cells from whole blood). Hence, it is also important to devise novel ways for the complementary elements of the system. Integration of micropumps and cell counters would lead to fully completed microchannel systems which are able to complete the process without using any external tool. Our research project has been oriented to focus on the development of the microchannels in that way, as we aim to produce integrated systems that can process real-life samples completely. Lastly, it is important to say that there are different microchannel cross section geometries presented recently [18], [19], [20].

By applying these designs to novel geometries, separation quality can be further enhanced since the hydrodynamic forces that arise in these geometries lead to better focus formation by using similar principles. Additionally, the single-layer microchannels can be manufactured into multiple-layered microchannels to increase the throughput up to hundreds of ml.min$^{-1}$ levels [21]. This ability of inertial microfluidics demonstrates its versatility, as such developments can be used in important applications in various fields such as desalination, filtration of potable water, and forensic sample processes.

## REFERENCES

[1]  M. Cristofanilli, G. T. Budd, M. J. Ellis, A. Stopeck, J. Matera M. C., Miller, ….. and D. F. Hayes, "Circulating tumor cells, disease progression, and survival in metastatic breast cancer," *New England Journal of Medicine*, vol. 351, no. 8, pp. 781-791, 2004.

[2]  H. W. Hou, M. E. Warkiani, B. L. Khoo, Z. R. Li, R. A. Soo, D. S. W. Tan, ... and C. T. Lim, "Isolation and retrieval of circulating tumor cells using centrifugal forces," *Scientific Reports*, vol. 3, pp. 1-8, 2013.

[3]  J. C. Giddings, "Field-flow fractionation: Analysis of macromolecular, colloidal, and particulate materials," *Science*, vol. 260, no. 5113, pp. 1456-1465, 1993.

[4]  M. Yamada, M. Nakashima and M. Seki, "Pinched flow fractionation: Continuous size separation of particles utilizing a laminar flow profile in a pinched microchannel," *Analytical Chemistry*, vol. 76, no. 18, pp. 5465-5471, 2004.

[5]  E. Chmela, R. Tijssen, M. T. Blom, H. J. Gardeniers and A. Van Den Berg, "A chip system for size separation of macromolecules and particles by hydrodynamic chromatography," *Analytical Chemistry*, vol. 74, no. 14, pp. 3470-3475, 2002.

[6]     X. Xu, K. K. Caswell, E. Tucker, S. Kabisatpathy, K. L. Brodhacker and W. A. Scrivens, "Size and shape separation of gold nanoparticles with preparative gel electrophoresis," *Journal of Chromatography A*, vol. 1167, no. 1, pp. 35-41, 2007.

[7]     M. Dürr, J. Kentsch, T. Müller, T. Schnelle and M. Stelzle, "Microdevices for manipulation and accumulation of micro-and nanoparticles by dielectrophoresis," *Electrophoresis*, vol. 24, no. 4, pp. 722-731, 2003.

[8]     C. Blattert, R. Jurischka, I. Tahhan, A. Schoth, P. Kerth and W. Menz, "Separation of blood in microchannel bends," In *Proceedings of the 26th Annual International Conference of the IEEE EMBS*, San Francisco, CA, U.S, 2004.

[9]     D. Di Carlo, D. Irimia, R. G. Tompkins and M. Toner, "Continuous inertial focusing, ordering, and separation of particles in microchannels," In *Proceedings of the National Academy of Sciences*, vol. 104, no. 48, pp. 18892-18897, 2007.

[10]    N. Pamme, "Continuous flow separations in microfluidic devices," *Lab on a Chip*, vol. 7, no. 12, pp. 1644-1659, 2007.

[11]    I. Gregoratto, C. J. McNeil and M. W. Reeks, "Micro-devices for rapid continuous separation of suspensions for use in micro-total-analysis-systems (µTAS)," In *MOEMS-MEMS 2007 Micro and Nanofabrication*. International Society for Optics and Photonics, California, CA, U.S, 2007.

[12]    D. Di Carlo, J. F. Edd, D. Irimia, R. G. Tompkins and M. Toner, "Equilibrium separation and filtration of particles using differential inertial focusing," *Analytical chemistry*, vol. 80, no. 6, pp. 2204-2211, 2008.

[13]    P. Patil, T. Kumeria, D. Losic and M. Kurkuri, "Isolation of circulating tumour cells by physical means in a microfluidic device: A review," *RSC Advances*, vol. 5, no. 109, pp. 89745-89762, 2015.

[14]    A. A. S. Bhagat, S. S. Kuntaegowdanahalli and I. Papautsky, "Continuous particle separation in spiral microchannels using dean flows and differential migration," *Lab on a Chip*, vol. 8, no. 11, pp. 1906-1914, 2008.

[15]    E. S. Asmolov, "The inertial lift on a spherical particle in a plane Poiseuille flow at large channel Reynolds number," *Journal of Fluid Mechanics*, vol. 381, pp. 63-87, 1999.

[16]    J. P. Beech and J. O. Tegenfeldt, "Tuneable separation in elastomeric microfluidics devices," *Lab on a Chip*, vol. 8, no. 5, 657-659, 2008.

[17]    S. S. Kuntaegowdanahalli, A. A. S. Bhagat, G. Kumar and I. Papautsky, "Inertial microfluidics for continuous particle separation in spiral microchannels," *Lab on a Chip*, vol. 9, no. 20, pp. 2973-2980, 2009.

[18]    M. E. Warkiani, A. K. P. Tay, G. Guan and J. Han, "Membrane-less microfiltration using inertial microfluidics," *Scientific Reports*, vol. 5, pp. 1-10, 2015.

[19]    L. Wu, G. Guan, H. W. Hou, A. A. S. Bhagat and J. Han, "Separation of leukocytes from blood using spiral channel with trapezoid cross-section," *Analytical Chemistry*, vol. 84, no. 21, pp. 9324-9331, 2012.

[20]    G. Guan, L. Wu, A. A. Bhagat, Z. Li, P. C. Chen, S. Chao, ... and J. Han, "Spiral microchannel with rectangular and trapezoidal cross-sections for size based particle separation," *Scientific reports*, vol. 3, pp. 1-9, 2013.

[21]    M. E. Warkiani, B. L. Khoo, L. Wu, A. K. P. Tay, A. A. S. Bhagat, J. Han and C. T. Lim, "Ultra-fast, label-free isolation of circulating tumor cells from blood using spiral microfluidics," *Nature Protocols*, vol. 11, no. 1, pp. 134-148, 2016.

— This article does not have any appendix. —